ECCOMAS

Proceedia

COMPDYN 2019
7th ECCOMAS Thematic Conference on
Computational Methods in Structural Dynamics and Earthquake Engineering
M. Papadrakakis, M. Fragiadakis (eds.)
Crete, Greece, 24–26 June 2019

CYCLIC NONLINEAR MODELING OF SEVERELY DAMAGED AND RETROFITTED REINFORCED CONCRETE STRUCTURES

George Markou¹, Christos Mourlas², Reyes Garcia³, Kypros Pilakoutas⁴, Manolis Papadrakakis²

¹ Department of Civil Engineering, University of Pretoria, South Africa e-mail: george.markou@up.ac.za

² Department of Civil Engineering, National Technical University of Athens, Greece {mourlasch, mpapadra}@central.ntua.gr

³ School of Engineering, The University of Warwick, UK reyes.garcia@warwick.ac.uk

⁴ Department of Civil and Structural Engineering, The University of Sheffield, UK k.pilakoutas@sheffield.ac.uk

Abstract

Advanced numerical methods for seismic assessment of existing substandard reinforced concrete (RC) structures have significantly evolved in the last two decades. Nonetheless, existing numerical tools have numerous limitations (e.g. numerical instabilities, applicable only in 1D or 2D problems, computationally demanding, etc.) and lack of objectivity and accuracy in providing robust, numerically accurate and objective solutions. As a result, new numerical approaches are necessary to solve some of these limitations.

This paper presents a detailed 3D modelling approach that solves some of the current modeling limitations. The approach is used to predict the experimental results from i) a substandard RC joint with inadequate detailing subjected to cyclic loading, and ii) the same RC joint rehabilitated and retrofitted with carbon fiber reinforced polymer (CFRP) sheets and subjected to cyclic loading. It is shown that the proposed numerical method reproduces the experimental results of both substandard and CFRP retrofitted specimens in a robust and computationally efficient manner. Current research is investigating the behavior of more RC components and full-scale retrofitted structures. This study contributes towards providing engineers and researchers with an advanced analytical tool to study the cyclic nonlinear behaviour of substandard RC structures.

Keywords: RC Joint, Nonlinear analysis, Finite Element Modelling, CFRP strengthening, deficient structures

ISSN:2623-3347 © 2019 The Authors. Published by Eccomas Proceedia. Peer-review under responsibility of the organizing committee of COMPDYN 2019. doi: 10.7712/120119.7127.18996

1 INTRODUCTION

Many numerical models have been proposed during the last decades for simulating the mechanical behavior of reinforced concrete (RC) structures. Nevertheless, a numerical approach combined with a constitutive model for concrete behavior that produces accurate and computationally efficient results for any RC structural member is still an open research subject. An accurate, objective and computationally efficient approach will constitute a powerful tool for any professional Civil Engineer and scientist that study the seismic performance of existing RC structures or perform the design of retrofitting interventions of severely damaged RC structures.

Many models that are found in the international literature can only describe certain aspects of the concrete material behavior and their implementation is limited to cases of small practical interest since they place emphasis on post-peak material characteristics, which are described by the introduction of several material parameters that have no physical meaning. A detailed literature review in regards to the modeling of RC structures can be found in [1, 2]. The numerical approach which was proposed in [1], is the latest research work that emphasizes on the ability of realistically predicting the behavior of concrete structures in a wide range of problems ranging from static cyclic to dynamic loading conditions, performed in a computationally efficient way.

The model that was proposed by Mourlas et al. [1], presents a numerical procedure which is based on the brittle nature of the material of concrete. The constitutive model is based on the experimental findings of Kotsovos and Newman [3] and a mathematical approach described in Kotsovos and Pavlovic [4]. This model is also used for the analysis of large-scale structures as described in Markou et al. [5], where a 4-storey RC building specimen was modeled through the Hybrid Modeling (HYMOD) approach [6, 7]. The under study RC building [5] was retrofitted with RC infill walls and carbon fiber reinforced polymer (CFRP) jacketing at its base, where three different load histories were applied until the frame reached its ultimate capacity. According to the HYMOD approach, the shear-dominated areas (RC joints, shear walls) are simulated by a detailed model that foresees the use of 8-noded hexahedral elements for discretizing the concrete domains and embedded beam elements for discretizing the steel reinforcement. The rest of the structure (bending dominated structural members) are modeled through the use of the beam-column finite element. It has to be noted here that in their work [5], the building was also retrofitted with RC infill walls and CFRP jacketing. Even though the proposed modeling method in [5] managed to capture the experimentally derived curves with high accuracy, the pinching effect was not reproduced accurately given that the concrete material deterioration (due to the multiple imposed cycles) and the potential rebar slippage at the base of the building were physical phenomena that were not numerically accounted for based on the adopted constitutive material models [1].

In this research article, a parametric investigation of a newly proposed material factor is performed, where it takes into account the loss of bond between the steel reinforcement and the surrounding damaged concrete, thus reduces the energy dissipation of the RC specimen's overall response based on the level of concrete damage. The methodology used in this research work foresees the validation of the proposed modeling method through the use of bare and retrofitted RC joints that were tested experimentally by Reyes et al. [8]. The numerically obtained P-δ curves are compared with both the experimental and numerical data in order to test the accuracy of the proposed method.

2 MATERIAL MODELING

2.1 Concrete Material Modeling and Damage Factor

The constitutive modelling of concrete has to describe a realistic behavior of concrete under generalized three dimensional states of stress as mathematically described in Kotsovos and Pavlovic [4]. The constitutive relations take the following form:

$$\varepsilon_0 = \varepsilon_{0(h)} + \varepsilon_{0(d)} = (\sigma_0 + \sigma_{id}) / (3K_s)$$
(1)

$$\gamma_0 = \gamma_{0(d)} = \tau_0 / (2G_s) \tag{2}$$

where K_s and G_s are the secant forms of bulk and shear moduli, respectively. The secant forms of bulk, shear modulus and σ_{id} are expressed as functions of the current state of stress which derived by regression analysis of the experimental data found in [3].

The model treats cracking with the smeared crack approach (see Fig. 1). In this way the models simulate the geometrical discontinuity by the assumption of displacement continuity. The crack opening strategy during each load increment foresees the use of the unified total crack approach (UTCA) proposed by Lykidis and Spiliopoulos [9], which foresees that the state of crack formation or closure is treated in a unified way within every Newton-Raphson internal iteration. When a crack is opened, the material properties normal to the crack plane are set to zero. The concrete material assumes that it loses all of its carrying capacity along the vertical direction of the crack, where it behaves in a brittle manner. The expression of the strength envelope of concrete is provided in Eq. 1 and it's based on the Willam and Warkne [10] formulae.

$$\tau_{0u} = \frac{2\tau_{0c}(\tau_{0c}^2 - \tau_{0e}^2)\cos\theta + \tau_{0c}(2\tau_{0e} - \tau_{0c})\sqrt{4(\tau_{0c}^2 - \tau_{0e}^2)\cos^2\theta + 5\tau_{0e}^2 - 4\tau_{0c}^2\tau_{0e}^2}}{4(\tau_{0c}^2 - \tau_{0e}^2)\cos^2\theta + (2\tau_{0e} - \tau_{0c})^2}$$
(3)

where the rotational variable θ defines the deviatoric stress orientation on the octahedral plane. The τ_{0e} (θ =0°) and τ_{0c} (θ =60°) correspond to the state of σ_1 = σ_2 > σ_3 (triaxial extension) and σ_1 > σ_2 = σ_3 (triaxial compression), respectively and are expressed analytically by experimental data.

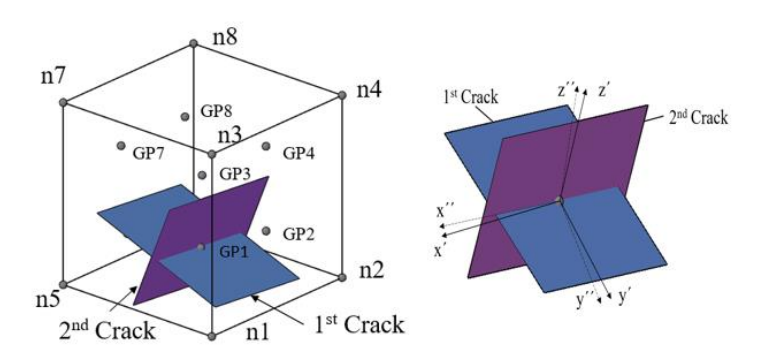


Figure 1: Local axes for the case of two cracks at a specific Gauss point. [5]

The material modeling procedure also uses a flexible crack closing criterion introduced in Mourlas et al. [1]. This numerical criterion was found to play a significant role during the cyclic loading analysis for achieving a faster convergence ratio. According to the proposed criterion in [1], the closure of cracks is expressed based on the following equation:

$$\varepsilon_{i} \leq a \cdot \varepsilon_{cr} = \left(b - \frac{n_{cr} - 1}{n_{tot}}\right) \cdot \varepsilon_{cr} \tag{4}$$

where ε_i is the current strain in the i-direction that is normal to the crack plane and ε_{cr} is the strain that causes cracking formation. Parameter b is the number of the imposed displacement branch of the load history, while n_{cr} and n_{tot} are the numbers of increment that the crack is formed at and the total number of increments that an imposed displacement branch is divided into, respectively.

When the criterion of crack-closure is satisfied at a Gauss Point, which had prior to that only one crack formation, then a part of the stiffness is lost along the previously crack plane (material deterioration) that was assumed to form in an orthogonal direction to the maximum principle tensile stress. Therefore, the constitutive matrix takes the following form:

$$C_{l}^{*} = \begin{bmatrix} a_{n} \cdot (1 - D_{c}) \cdot (2G_{t} + \mu) & a_{n} \cdot (1 - D_{c}) \cdot \mu & a_{n} \cdot (1 - D_{c}) \cdot \mu & 0 & 0 & 0 \\ a_{n} \cdot (1 - D_{c}) \cdot \mu & a_{n} \cdot (1 - D_{c}) \cdot (2G_{t} + \mu) & a_{n} \cdot (1 - D_{c}) \cdot \mu & 0 & 0 & 0 \\ a_{n} \cdot (1 - D_{c}) \cdot \mu & a_{n} \cdot (1 - D_{c}) \cdot \mu & 2G_{t} + \mu & 0 & 0 & 0 \\ 0 & 0 & 0 & a_{s} \cdot (1 - D_{c}) \cdot \beta \cdot G_{t} & 0 & 0 \\ 0 & 0 & 0 & 0 & a_{s} \cdot (1 - D_{c}) \cdot \beta \cdot G_{t} & 0 \\ 0 & 0 & 0 & 0 & 0 & a_{s} \cdot (1 - D_{c}) \cdot \beta \cdot G_{t} \end{bmatrix}$$

$$(5)$$

where β is a shear retention factor, a_n and a_s are constants with recommended values of 0.25 and 0.125, respectively, based on the parametric investigation presented in [11]. The proposed expressions of the constitutive matrix describes the anisotropic behavior of concrete at the local coordinate system, therefore, it has to be transformed to the global system by using the standard coordinate system transformation laws as follows:

$$C_{o} = T^{T} C_{I} T \tag{6}$$

where T is the transformation matrix consisted by the direction cosines that define the relative orientation of the local to global axis. The factor D_c is a damage factor proposed in [11], describing the accumulated energy loss due to the number of times a crack has opened and closed. As it was suggested in [11], the damage factor has the following form:

$$D_{c} = e^{-(1-a)/f_{cc}} = e^{-\left(1-\left(1-\frac{\varepsilon_{cr}}{\varepsilon_{\max}}\right)\right)/f_{cc}} = e^{-\left(\frac{\varepsilon_{cr}}{\varepsilon_{\max}}\right)/f_{cc}}$$
(7)

where f_{cc} is the number of times where a crack has closed and is updated in every iteration at every Gauss Point. A schematic representation of Eq. 7 can be seen in Fig. 2.

During the nonlinear analysis, the constitutive matrix is calculate according to Eq. 5 when a crack is closed at a Gauss point, which had previously one or two cracks. After the crack closure, the stresses are corrected through the use of the following expression:

$$\sigma^{i} = \sigma^{i-1} + C_{g} \cdot \Delta \varepsilon^{i} \tag{8}$$

Finally, when all the cracks have been closed (of a previously cracked Gauss Point) and the reduction factor a (Eq. 4) of one of the previous cracks is larger than 0.5, then the constitutive matrix takes the following form:

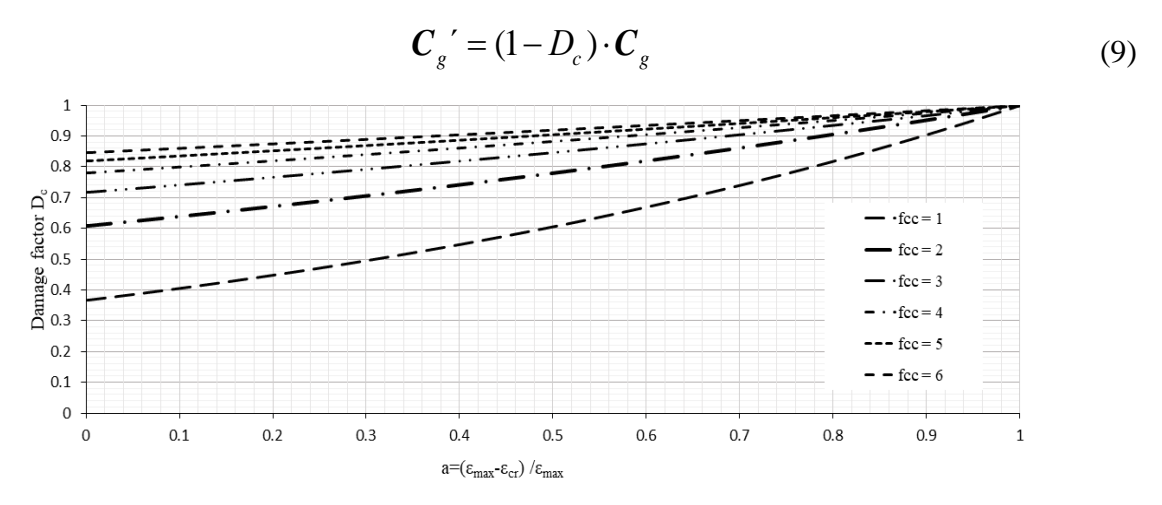


Figure 2: Schematic representation of the damage factor D_c (Eq. 7) as a function of the parameter a and f_{cc} . [11]

2.2 Steel Material Modeling and Modified Damage Factor

According to any nonlinear behavior of cracked RC structural members, the level of damage that occurs due to the opening of cracks affects the respective contribution of the steel reinforcement to the surrounding concrete areas. Consequently, the cracks directly affect the internal force transfer mechanism from the rebars to the surrounding concrete domain, especially in the anchorage areas. Therefore, a modification of the steel stress-strain relation of Menegotto-Pinto [12] is proposed herein that is related to the level of concrete cracking surrounding the rebar element during the nonlinear cyclic analysis. The loss of bonding between steel reinforcement with the surrounding cracked concrete can indirectly be taken into account by reducing the stiffness contribution of steel reinforcement [11], thus simulate the pinching effect. Hence, the introduction of a bond-slip model, which will require the definition of new material parameters and an additional dof at each reinforcement bar, can be avoided.

Based on the proposed formulation presented in [11], the average of all parameters *a* (found in Eqs. 4 and 10, and expressed by Eq. 11) at the 8 Gauss Points of any concrete hexahedral element can be used to determine the level of damage of the concrete material as expressed through Eq. 10.

$$D_s = \left[1 - a_{Element}\right] \tag{10}$$

where,

$$a_{Element} = \frac{\sum_{i=1}^{ncr} a_i}{ncr}, ncr \text{ is the number of cracked Gauss Points}$$
 (11)

In the case of unloading, when the structure reaches its initial deformation, a material deterioration of the steel reinforcement is computed based on the following proposed formulae:

$$E_{s}' = (1 - D_{s})E_{s} \tag{12}$$

The material deterioration is applied when the criterion $\sigma_s \cdot \epsilon_s < 0$ is satisfied, which describes the situations when crack closures and re-openings occur, where the pinching phenomena are excessive.

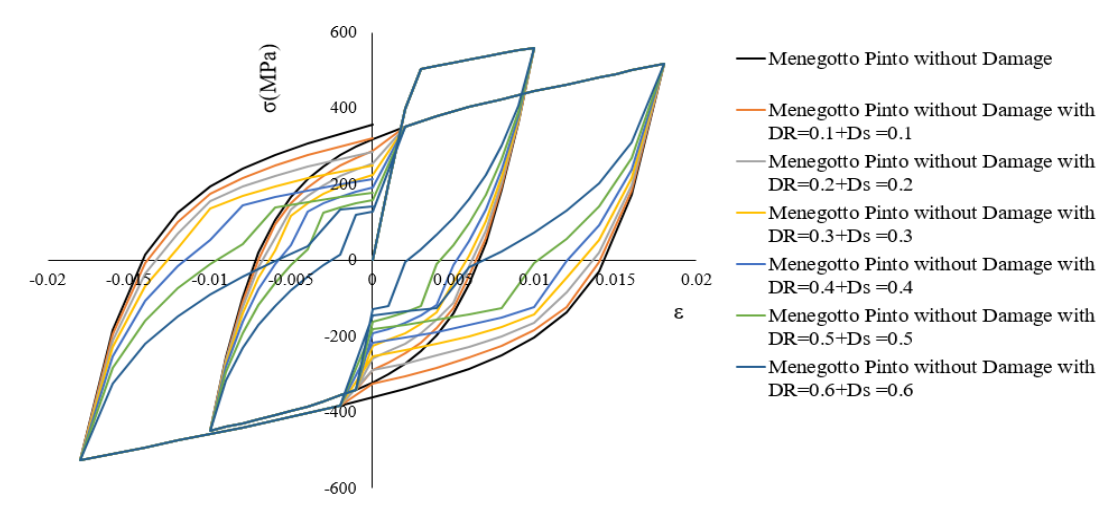


Figure 3: Menegotto-Pinto steel model that uses the modified formulation for parameters E'(Eq. 12) and R'(Eq. 14) with different values of the damage factor D_R and D_S .

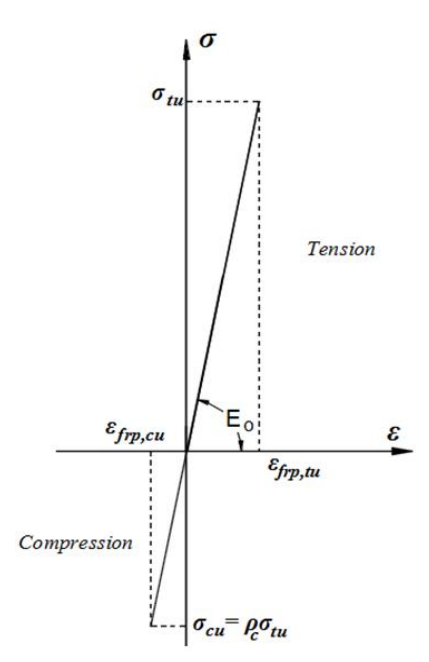


Figure 4: Material model of the CFRP jacketing. [13]

Additionally, so as to capture the pinching effect at a material level, the reduction of parameter *R* (see Eq. 13) of the Menegotto-Pinto [12] model is proposed.

$$R = R_0 - \frac{a_1 \xi}{\alpha_2 + \xi} \tag{13}$$

It must be noted here that R_0 , a_1 and a_2 are experimentally determined parameters and assumed to be 20, 18.5 and 0.15, respectively, in this study. By using the same concept de-

scribed above, the reduction factor D_R is proposed in order to decrease the parameter R into R' which is calculated though the following expression:

$$R' = (1 - D_R)R$$
, where $D_R = D_s$ (14)

The material deterioration is once more applied when the criterion $\sigma_s \cdot \varepsilon_s < 0$ is satisfied. The modified Menegotto-Pinto material model's numerical response is illustrated in Fig. 3, according to the proposed formulation. Before moving to the next section, it is noteworthy to state at this point that the material model used to simulate the stress-strain relationship of the CFRP jacketing foresaw a linear behavior until complete failure for both tension and compression states, as shown in Fig. 4. As it can be seen, it was assumed that when the ultimate stress level at any Gauss Point of the CFRP hexahedral elements was reached, the model foresees for a complete loss of its capacity. According to the reported material properties [8], the ultimate CFRP tensile strength was set to 4,140 MPa and the Young Modulus of elasticity was set equal to 241 GPa. In addition to that, it was also assumed that the CFRP hexahedral elements that were used to discretize in detail the jacketing, had full bonding with the concrete finite elements.

3 NUMERICAL IMPLEMENTATION

The numerical investigation foresaw the use of finite element meshes that will be described in this section, followed by a discussion on the obtained numerical findings. All analyses were performed by using a displacement control algorithm that adopted an energy convergence criterion expressed in Eq. 15. The energy convergence tolerance was set equal to 10^{-5} , whereas the CPU used to perform all the analyses presented in this section, had a 3.7 GHz computing power.

$$e_{err} = \frac{\Delta u_s^j \left\| F_s^{t+\Delta t} - R_s^{t+\Delta t} \right\|}{\Delta u_s^l \left\| F_s^{t+\Delta t} - R_s^t \right\|} \le tolerance$$
(15)

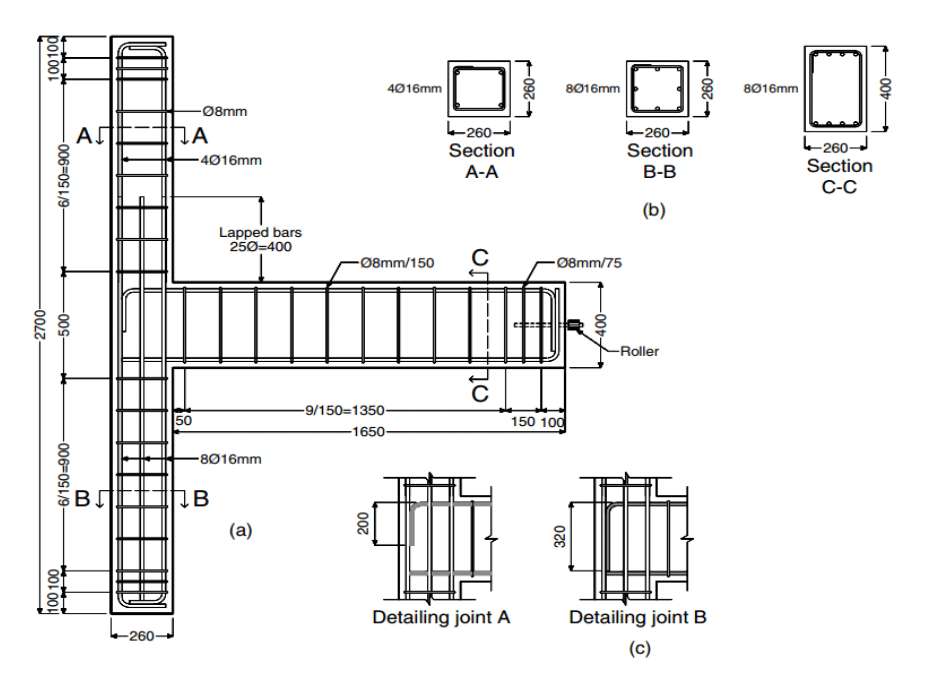


Figure 5: Geometric and reinforcement details of the beam-column joints tested in Garcia et al. [8].

The numerical implementation foresaw the study of an exterior joint that was tested by Garcia et al. [8] under extreme cyclic loading (see Fig. 5). The column had a cross-section of 260 x 260 mm and the longitudinal reinforcement were 16 mm in diameter. The beam was designed to have a cross section of 260x400 mm and was also reinforced with 16 mm rebars, as it can be depicted in Fig. 5.

Two types of bar anchorage detailing were examined for the top beam reinforcement as shown in Fig. 5. The beam reinforcement of type A and B (Fig. 5c) were anchored into the joint for a length of 220 mm (approximately $14d_b$) without foreseeing for any hooks nor bends. This short anchorage was designed to be insufficient in order to develop slippage, thus extreme nonlinearities within the joint volume. Furthermore, the flexural strength of the RC column was designed to be the same as the beam's, a design strategy that does not follow the modern design philosophy that foresees a strong column-weak beam approach. The specimens were designed to fail at the core, where there are no confining stirrups to provide the joint with the ability to behave in a ductile manner. In order to avoid the shear failure outside the core of the joint, 8 mm transverse stirrups were provided at both column and the beam members spaced every 150 mm. The mean concrete compressive strength was reported to be 32 MPa and 31.3 MPa for specimens JA2 and JB2, respectively, where the respective tensile splitting strength was 2.44 MPa and 2.41 MPa for the two specimens, respectively. The yield and tensile strength of the steel reinforcement were reported to be $f_v = 612$ MPa and $f_u = 726$ MPa for the 8 mm rebars and $f_y = 551$ MPa and $f_u = 683$ MPa for the 16 mm rebars. Additionally, the elastic modulus was found [8] to be equal to $E_s = 209$ GPa.

The frame joints were subjected to different cyclic loading sets according to the experiment's setup. The initial loading history applied on the bare specimens consisted of three push-pull cycles at drift ratios of $\pm 0.25\%$, $\pm 0.5\%$, $\pm 0.75\%$, $\pm 1.0\%$, $\pm 1.5\%$, $\pm 2.0\%$, $\pm 3.0\%$, $\pm 4.0\%$ and $\pm 5.0\%$. Furthermore, a second actuator applied a constant axial load equal to N = 150 kN on the column as illustrated in Fig. 6.

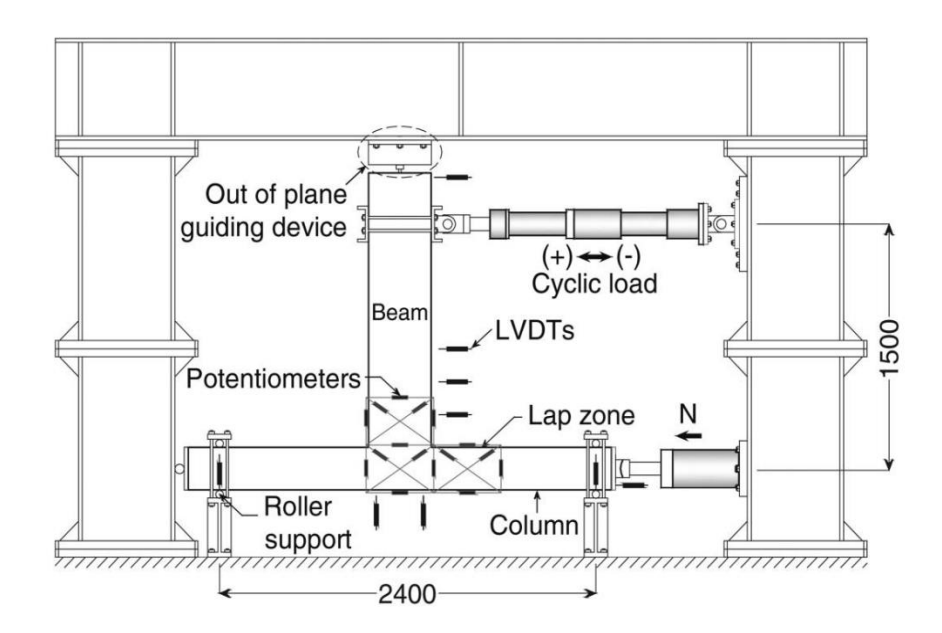


Figure 6: Test setup (units: mm) and instrumentation of RC joints. [8]

According to the experimental results reported in [8], the bare specimens suffered from severe damages, where excessive diagonal cracking and partial concrete spalling at the region of the core had been observed, as shown in Fig. 7.

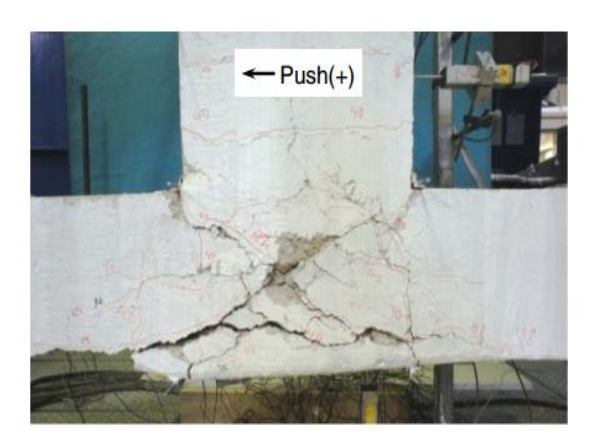


Figure 7: Crack patterns after the failure of JB2 bare RC specimen. [8]

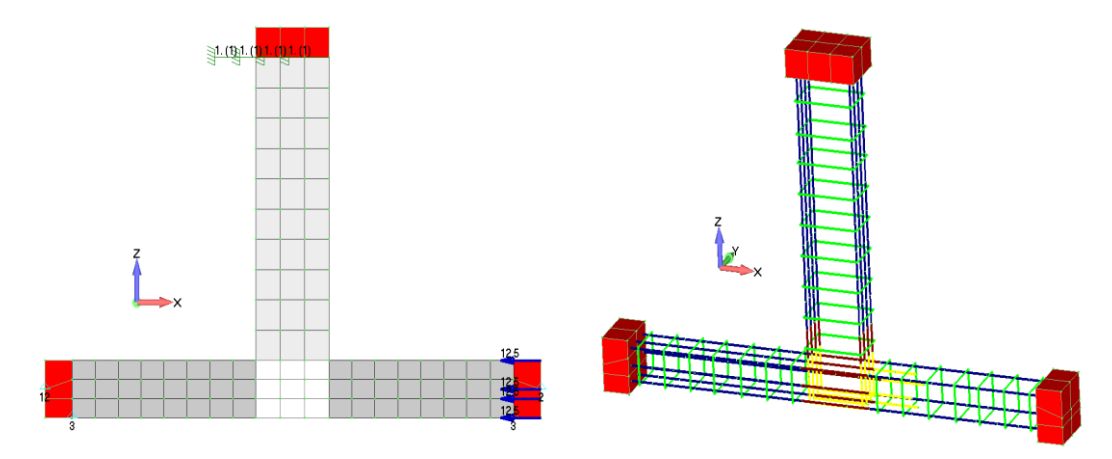


Figure 8: RC joint JB2. (Left) Hexahedral and (Right) embedded rebar finite element meshes.

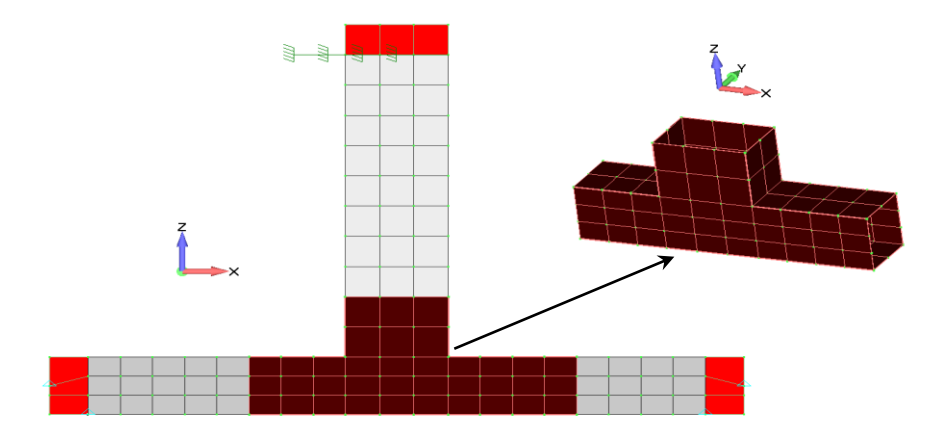


Figure 9: Retrofitted RC joint JB2RF. Concrete and CFRP hexahedral finite element meshes.

For the needs of this research work, specimen JB2 was studied through the use of the proposed numerical model that uses the damage factors for concrete and steel reinforcement, as presented in section 2.2. So as to study the mechanical behavior of specimen JB2, the concrete domain was discretized with 8-noded hexahedral finite elements and the steel reinforcement.

forcement was discretized with Natural Beam-Column Flexibility-Based elements [14]. A total number of 174 concrete and 324 steel elements were used to discretize the RC joint, where 18 hexahedral steel elements (red color) were used at the areas of the boundary conditions in order to prevent local failure (see Fig. 8). Furthermore, for the retrofitted RC joint (JB2RF), 156 hexahedral elements were used for the CFRP jacketing as shown in Fig. 9. The FE mesh and material details for both RC joints are given in Tables 1 and 2, respectively.

a/a	Model	Total Number of Nodes	Hexahedral Elements	Embedded Rebar Elements	
1	JB2	396	192	500	
2	JB2RF	620	348	500	

Table 1: FE mesh details of the two RC Joint models.

Material	Young Modulus (GPa)	Hardening Modulus (GPa)	Yielding Stress / Tensile Strength* (MPa)	Compressive Strength (MPa)	Shear remaining strength β	Poisson Ratio	Ultimate Strain ε
Concrete	20	-	2.41*	31.3	0.03	0.2	-
High Strength Concrete	30	-	3.91*	55.3	0.05	0.2	-
Steel Rebars	190	1	551 (Ø16) / 612 (Ø8)	-	-	0.3	15%
CFRP	50	-	300*	-	-	0.3	0.6%

Table 2: Material details used in the FE model.

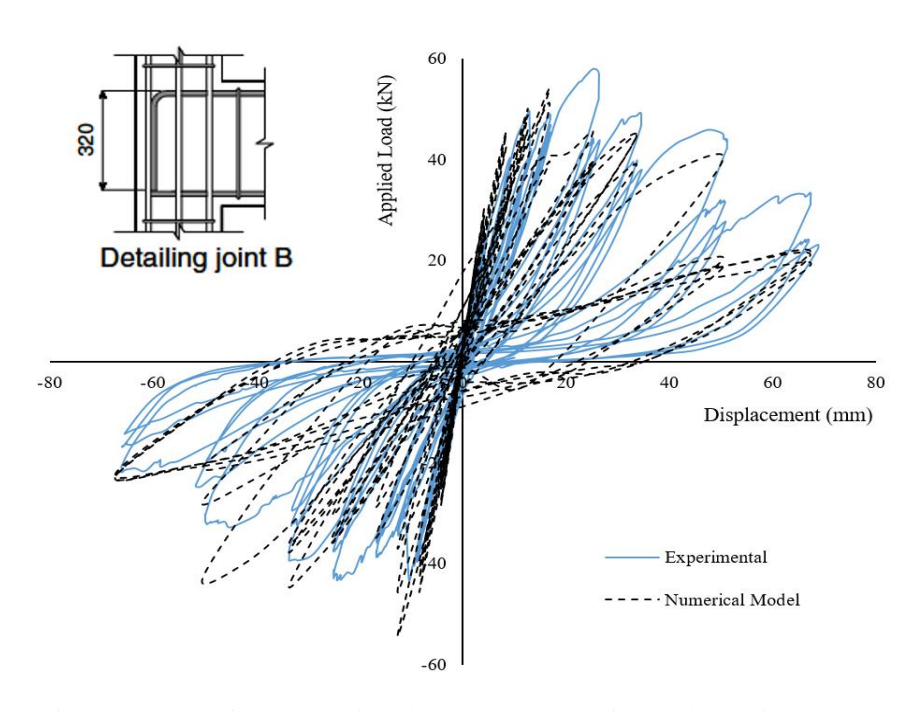


Figure 10: JB2 Joint. Comparison between the numerical and experimental curves.

The computed force-displacement curves for the two specimens (JB2 and JB2FR) are compared with the corresponding experimental data in Figs. 10 and 11, respectively. As it can be seen, the numerical results match very well with the experimental data, where the stiffness and the resulted load-carrying capacity of the specimen were predicted in an accurate manner. The numerical results show that the concrete damage factors managed to capture the stiffness

and load-capacity degradation, where the pinching characteristics for both specimens were described with an acceptable accuracy. It is evident that the proposed modeling approach manages to captured this highly complicated physical phenomenon through the use of the modified Menegotto-Pinto model and by adopting the proposed damage factors D_S and D_R given in section 2.2 by Eqs. 10 and 11, respectively.

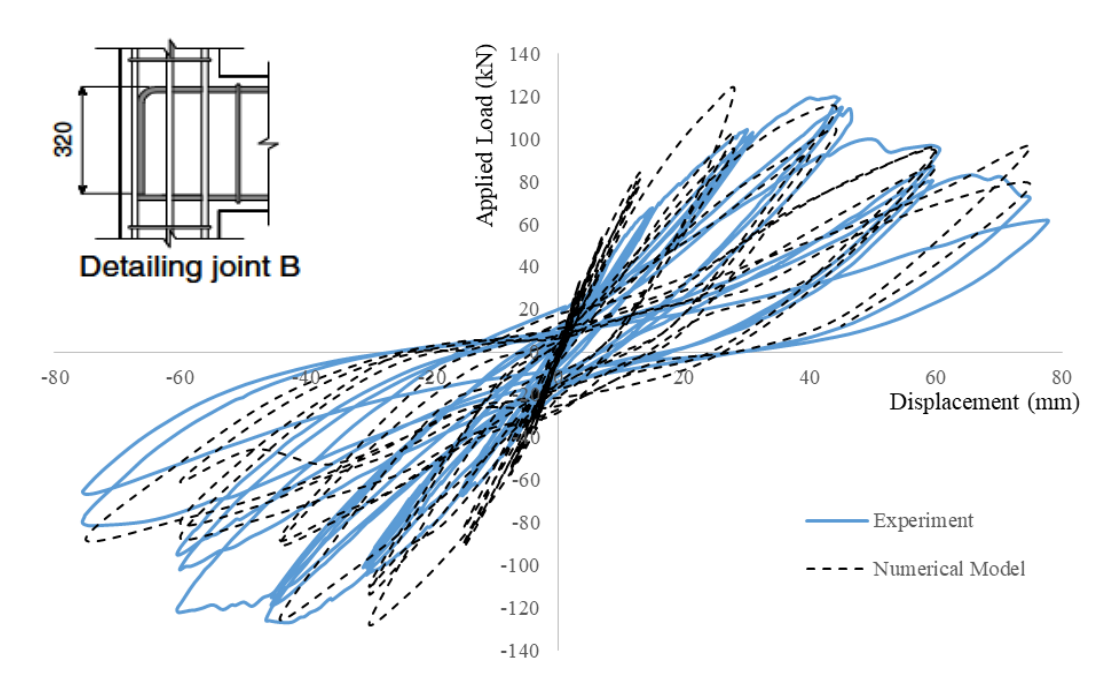


Figure 11: JB2FR Joint. Comparison between the numerical and experimental curves.

According to the numerical findings, the FE model developed for simulating the retrofitted specimen JB2FR not only managed to capture numerically the hysteretic behavior of the specimen and its strength's corresponding degradation, but it was also able to predict the stiffness degradation of a structural joint that foresaw three different solid domains:

- a. Old damaged concrete,
- b. New high-strength concrete found in the joint and
- c. CFRP jacketing.

It must be noted herein that the numerical analysis failed to converge during the final cycle of imposed displacements due to excessive cracking of the concrete domain within the joint domain. Finally, the proposed numerical model for the case of the retrofitted specimen was able to predict the overall strength enhancement with a deviation that was less than 5%.

4 CONCLUSIONS

In this research work, a 3D detailed modeling approach is used for the simulation of bare and CFRP retrofitted RC joints. The proposed numerical model has been integrated with a newly proposed damage factor for the steel material that is directly connected to the number of opening and closing of concrete cracks that occurs during the nonlinear analysis. This damage factor, which is an extension of the damage factor proposed in [11], was developed to account the loss of bonding between steel reinforcement and the cracked surrounding concrete within areas that are expected to undergo significant cracking.

According to the numerical investigation's findings, the proposed model managed to capture the hysteretic behavior of both the bare and CFRP retrofitted RC joints, which were subjected to ultimate limit cyclic loading conditions. The modification of the steel reinforcement model was able to reproduce the severe pinching effects that occurred during the cyclic loading of the bare joint. Additionally, the corresponding extreme pinching effect of the retrofitted RC joint was also numerically reproduced with an acceptable accuracy, where the numerical and experimental curves were found to be in a good agreement. Furthermore, for the case of the CFRP retrofitted specimen, the proposed modeling approach managed to reproduce the overall strength enhancement of the joint with an accuracy that foresaw a deviation of less than 5% compared to the experimental data.

Future research work foresees the implementation of the proposed algorithm in predicting the mechanical behavior of additional specimens that are characterized by extreme pinching phenomena, while use the developed technology in the parametric investigation of the mechanical response of full-scale structures that undergo extreme cyclic loading. Finally, the proposed modeling approach will be used for the study of the effects that different interventions derive in-terms of the overall mechanical behavior and strength enhancement of RC structural framing systems.

REFERENCES

- [1] Mourlas C., Papadrakakis M., Markou G. A computationally efficient model for the cyclic behavior of reinforced concrete structural members. Engineering Structures, Vol. 141, pp. 97–125, 2017.
- [2] Lykidis G.C., Spiliopoulos K.V. An efficient numerical simulation of the cyclic loading experiments on RC structures. Computers and Concrete, Vol. 13(3), pp. 343–59, 2014.
- [3] Kotsovos M.D., Newman J.B.. Behavior of Concrete Under Multiaxial Stress. ACI Journal Proceedings, Vol. 74(9), pp. 213–23, 1977.
- [4] Kotsovos M.D., Pavlovic M. Structural concrete: finite-element analysis for limit-state design. T. Telford; 1995.
- [5] Markou G., Mourlas C., Bark H., Papadrakakis M. Simplified HYMOD non-linear simulations of a full-scale multistory retrofitted RC structure that undergoes multiple cyclic excitations An infill RC wall retrofitting study. Engineering Structures, Vol. 176, pp. 892–916, 2018.
- [6] Markou G., Papadrakakis M. A simplified and efficient hybrid finite element model (HYMOD) for non-linear 3D simulation of RC structures. Engineering Computations, Vol. 32(5), pp. 1477–524, 2015.
- [7] Markou G., Mourlas C., Papadrakakis M. Computationally Efficient and Robust Nonlinear 3D Cyclic Modeling of RC Structures Through a Hybrid Finite Element Model (HYMOD). International Journal of Computational Methods, 2018.
- [8] Garcia R., Jemaa Y., Helal Y., Guadagnini M., Pilakoutas K. Seismic Strengthening of Severely Damaged Beam-Column RC Joints Using CFRP. Journal of Composites for Construction, Vol. 18(2), pp. 04013048, 2014.
- [9] Spiliopoulos K.V., Lykidis G.C. An efficient three-dimensional solid finite element dynamic analysis of reinforced concrete structures. Earthquake Engineering & Structural Dynamics, Vol. 35(2), pp. 137–57, 2006.
- [10] Willam K., Warnke E.P. Constitutive model for the triaxial behavior of concrete. Seminar on concrete structures subjected to triaxial stresses, Instituto Sperimentale Modeli e Strutture, Bergamo, Paper III-1., 1974.
- [11] Mourlas C., Markou G., Papadrakakis M. Accurate and computationally efficient nonlinear

- static and dynamic analysis of reinforced concrete structures considering damage factors. Engineering Structures, Vol. 178, pp. 258–85, 2019.
- [12] Menegotto M., Pinto P.E. Method of analysis for cyclically loaded reinforced concrete plane frames including changes in geometry and non-elastic behavior of elements under combined normal force and bending. Proceedings, IABSE Symposium on Resistance and Ultimate Deformability of Structures Acted on by Well Defined Repeated Loads, Lisbon, Portugal, 15–22., 1973.
- [13] Markou, G., AlHamaydeh, M. (2018), 3D Finite Element Modeling of GFRP-Reinforced Concrete Deep Beams without Shear Reinforcement, International Journal of Computational Methods, 15(1), pp. 1-35.
- [14] Markou, G., Papadrakakis, M., "Accurate and Computationally Efficient 3D Finite Element Modeling of RC Structures", Computers & Concrete, 12 (4), pp. 443-498, 2013.